Machine learning of large-scale multimodal brain imaging data reveals neural correlates of hand preference

Pattarawat Chormai [b,c,d], Yi Pu [e], Haoyu Hu [a], Simon E. Fisher [d,f], Clyde Francks [d,f,g,1], Xiang-Zhen Kong [a,d,h,*]

[a] Department of Psychology and Behavioral Sciences, Zhejiang University, Hangzhou, China
[b] Technische Universität Berlin, Germany
[c] Max Planck School of Cognition, Max Planck Institute of Human Cognitive and Brain Sciences, Leipzig, Germany
[d] Language and Genetics Department, Max Planck Institute for Psycholinguistics, Nijmegen, The Netherlands
[e] Department of Neuroscience, Max Planck Institute for Empirical Aesthetics, Frankfurt am Main, Germany
[f] Donders Institute for Brain, Cognition and Behaviour, Radboud University, Nijmegen, The Netherlands
[g] Department of Human Genetics, Radboud University Medical Center, Nijmegen, the Netherlands
[h] Department of Psychiatry of Sir Run Shaw Hospital, Zhejiang University School of Medicine, Hangzhou, China

ARTICLE INFO

ABSTRACT

Lateralization is a fundamental characteristic of many behaviors and the organization of the brain, and atypical lateralization has been suggested to be linked to various brain-related disorders such as autism and schizophrenia. Right-handedness is one of the most prominent markers of human behavioural lateralization, yet its neurobiological basis remains to be determined. Here, we present a large-scale analysis of handedness, as measured by self-reported direction of hand preference, and its variability related to brain structural and functional organization in the UK Biobank ($N = 36,024$). A multivariate machine learning approach with multi-modalities of brain imaging data was adopted, to reveal how well brain imaging features could predict individual's handedness (i.e., right-handedness vs. non-right-handedness) and further identify the top brain signatures that contributed to the prediction. Overall, the results showed a good prediction performance, with an area under the receiver operating characteristic curve (AUROC) score of up to 0.72, driven largely by resting-state functional measures. Virtual lesion analysis and large-scale decoding analysis suggested that the brain networks with the highest importance in the prediction showed functional relevance to hand movement and several higher-level cognitive functions including language, arithmetic, and social interaction. Genetic analyses of contributions of common DNA polymorphisms to the imaging-derived handedness prediction score showed a significant heritability (h^2=7.55%, p <0.001) that was similar to and slightly higher than that for the behavioural measure itself (h^2=6.74%, p <0.001). The genetic correlation between the two was high (r_g=0.71), suggesting that the imaging-derived score could be used as a surrogate in genetic studies where the behavioural measure is not available. This large-scale study using multimodal brain imaging and multivariate machine learning has shed new light on the neural correlates of human handedness.

Introduction

Lateralization is a fundamental characteristic of many behaviours and cognitive functions in human beings (Karolis et al., 2019; Kong et al., 2020a; McManus 2022; Toga and Thompson, 2003). Among them, the most researched and prominent example of lateralization is human handedness laterality. Many tests have been proposed for assessing one's handedness, including the Edinburgh Handedness Inventory for hand preference test (Oldfield, 1971) and the Annett pegboard

for asymmetry of hand skill (Annett, 1970). In the general population roughly 90% of people are right-handed, and 10% left-handed (de Kovel and Francks, 2019; Peters et al., 2006; Papadatou-Pastou et al., 2020; Kong et al., 2021). As a striking example of lateralization, handedness has drawn great attention in fields including psychology, psychiatry, neuroscience, and human evolution. For example, handedness has been claimed to be associated with personality (Mascie-Taylor, 1981), cognitive skills such as language (Corballis, 2003), and psychiatric disorder such as attention deficit hyperactivity disorder (ADHD) (Nastou et al.,

2022) and depression (Logue et al., 2015; cf. Packheiser et al., 2021). Non-right-handedness has also been suggested to be linked to early life factors (de Kovel and Francks, 2019; Kong et al., 2021) and various neurodevelopmental and psychiatric disorders, such as autism (Markou et al., 2017) and schizophrenia (Hirnstein and Hugdahl, 2014). However, these data are mostly correlational, and the neurobiological basis of handedness remains elusive.

In general, variation in handedness is thought to reflect differences in the functional and structural organization of the human brain (Toga and Thompson, 2003). This idea has been tested many times, particularly in the context of recent advances in neuroimaging methods. Results on the association between handedness and brain measures have mostly been equivocal, likely due to limited effect sizes of each single imaging modality in the context of relatively small samples (Kong and Francks, 2022), as well as differences in scanning and image processing. Structurally, while some studies reported significant associations (Germann et al., 2019; Guadalupe et al., 2014; Marie et al., 2015), others reported that handedness has little to do with gray matter asymmetries in volume, cortical thickness, surface areas, or sulcal depth (Kong et al., 2018; Maingault et al., 2016)(Carrion-Castillo, 2020). In terms of white matter anatomy, structural connectivity of some intra- (e.g., superior longitudinal fasciculus) and inter-hemispheric (i.e., corpus callosum) pathways seems to differ between left- and right-handers, but inconsistent evidence also exists (Budisavljevic et al., 2020). Functionally, various differences in brain activity related to motor control have been observed between left- and right-handers (Tzourio-Mazoyer et al., 2021). It has also been proposed that leftward language hemispheric lateralization was closely linked to the evolution of population-level right-handedness (Corballis, 2003), although studies have found that the relationship in terms of inter-individual variation is weak and complex (Mazoyer et al., 2014). Besides the motor control and language-related lateralization, task fMRI has indicated that handedness is related to lateralization of the core face perception network (i.e., the fusiform face area) and pointed to different neural mechanisms underlying face processing in left- and right-handers, suggesting a broader and complex underlying process regulating brain lateralization (Frässle et al., 2016).

Recently, thanks to the large-scale and high-quality UK Biobank dataset, researchers have begun to study potential brain-handedness associations using larger sample sizes. One study using this sample (N >40,000) clarified the relationship between handedness and overall brain skew (torque in the horizontal and vertical planes (Kong et al., 2021), and another study of cortex-wide asymmetries (N >31,000) showed significant (but small) differences between left-handers and right-handers in regions important for hand control, language, vision, and working memory (Sha et al., 2021). A resting-state fMRI study in the UK Biobank (N =~9000) showed significant association with functional connectivity between pairs of resting-state networks, particularly for the left and right (homologous) language networks (Wiberg et al., 2019). However, it is important to note that these previous large-scale studies used univariate approaches, without attempting to integrate information from both structural and functional measures (indeed two of them only investigated structural measures). The effect sizes of the associations revealed in these studies were low (e.g., Cohen's d <0.10 or correlation r <0.10) (Kong et al., 2021; Sha et al., 2021; Wiberg et al., 2019). While these large-scale neurobiological studies in the UK Biobank have indicated various neural correlates of handedness with a degree of precision and statistical reliability that was previously not possible, the small effect sizes suggest that a large-scale survey that integrates various modalities of brain imaging data and assembles the small effects may be a major step forward for establishing a more robust brain-behavior association and understanding the neurobiological basis of handedness.

In principle, machine learning techniques might allow us to build multivariate predictive models for behavior which are able to capture effects of high-dimensional features and multimodalities of brain imaging data (Bzdok and Meyer-Lindenberg, 2018; Li et al., 2022; Marek et al., 2022). In other words, by applying machine learning to big data com-

prising brain and behavioural measures, we could clarify whether and to what extent models of brain imaging data can predict individual behavior, such as handedness preference. Moreover, such predictive models could also enhance our understanding of the neurobiology of behavior by identifying the most important features, as well as the networks consisting of these features, in the prediction. In addition, a predictive model could provide an imaging-derived score which could serve as a proxy of a behavioural measure, for example to enable future large-scale cognitive neuroimaging genetics studies when only brain imaging data but no behavioural data was collected.

Towards this goal, Panta et al. provided an initial attempt to classify handedness with structural MRI data from less than 200 participants, and achieved a prediction accuracy of up to 80% (Panta et al., 2021). With a newly proposed BigFLICA decomposition method which integrates data compression techniques and linked independent component analysis approach, Gong et al. identified a multimodal mode (a.k.a., independent component) which showed a correlation of $r = 0.23$ with handedness in the UK Biobank ($N = 14,503$) (Gong et al., 2021). The present study aimed to explicitly model the associations between handedness, as measured by self-reported direction of hand preference, and multimodal brain variables using a machine learning approach, and represents the largest-ever analysis of handedness and its variability related to brain structural and functional organization, using the UK Biobank ($N = 36,024$). We used a machine learning approach with multiple modalities of brain imaging data to investigate the relationship between handedness and the human brain, and to further identify key features that are associated with handedness (i.e., right-handedness vs. non-right handedness). In addition, we made use of the best predictive model and derived a continuous score as a metric of probability of each individual being right-handed, and confirmed that such an imaging-derived handedness score could be useful for follow-up studies on the biology of handedness.

Materials and methods

Datasets

Data were obtained from the UK Biobank as part of research application 16,066. This is a general adult population cohort. The data collection in the UK Biobank, including the consent procedure, has been described elsewhere (Alfaro-Almagro et al., 2018; Bycroft et al., 2018; (Sudlow et al., 2015)). Informed consent was obtained for all participants, and the UK Biobank received ethical approval from the National Research Ethics Service Committee North West - Haydock (reference 11/NW/0382). For this study, we used data from the February 2020 release and excluded the withdrawn participants as announced by the UK Biobank in August 2021. A subset of participants was included in this study for whom the handedness and brain imaging data were available, and in total, this subset had 36,024 participants. The median age of these participants was 64 years, range 45–81 years, and 19,171 (53%) subjects were female.

Brain imaging modalities

All of the brain imaging features used in the analyses were derived and made available from the neuroimage processing pipeline of the UK Biobank (Alfaro-Almagro et al., 2018;(Miller et al., 2016)). These features included the following imaging modalities:

Structure MRI: Features in this category were derived from the parcellation of the cortex using the Desikan-Killiany atlas and Freesurfer (Fischl, 2012). These features were area, volume, and mean thickness of regions in the Desikan-Killiany atlas in both hemispheres. We did not use each hemisphere's total cortical surface area or overall mean cortical thickness in our analysis.

Diffusion MRI Skeleton: This modality contains several diffusion metrics in each area of the brain based on tract-skeleton processing on

Table 1

Groups of features used for training multivariate machine learning models. Each group contains a different number of features, and its UK Biobank reference is indicated.

Feature Group	Number of Features	UK Biobank Reference
Structure MRI (S)	198	Category 192
Diffusion MRI Skeleton (D)	432	Category 134
rfMRI Component Amplitudes (CA-25)	21	Field 25,754
rfMRI Component Amplitudes (CA-100)	55	Field 25,755
rfMRI Full Correlation Matrix (FC-25)	210	Field 25,750
rfMRI Full Correlation Matrix (FC-100)	1485	Field 25,751
rfMRI Partial Correlation Matrix (PC-25)	210	Field 25,752
rfMRI Partial Correlation Matrix (PC-100)	1485	Field 25,753

Table 2

Controlled features and their UK Biobank references.

Controlled Feature Group	UK Biobank Reference
Sex	f.31.0.0
Age	f.21003.2.0
Genetic PCs	f.22009.0.[0–10]
Imaging assessment center	f.54.2.0
Scanner-position-{x, y, z}	f.2575[6–8].2.0
Signal-to-noise in T1	f.25734.2.0
dMRI outlier slices detected and corrected	f.25746.2.0
Resting-State fMRI head motion	f.25741.2.0
Resting-State Signal to Noise	f.25744.2.0

fractional anisotropy (FA) images in a standard white-matter skeleton space. Such metrics were fractional anisotropy, intra-cellular volume fraction (ICVF), isotropic free water volume fraction (ISOVF), mean diffusivity, anisotropy mode (MO), and orientation dispersion (OD).

Resting-State fMRI: This modality is based on blood-oxygen signals in the brain. These signals are considered as measures of the brain's intrinsic activities and can be used to estimate the functional level of connectivity between different brain regions (Canario et al., 2021; Kong et al., 2017). As described by (Alfaro-Almagro et al., 2018), features were extracted and provided in a form of components from independent component analysis (Hyvärinen and Oja, 2000); two numbers of independent components (ICs) are used, namely 25 and 100. Components that were identified as artefacts were removed by the UK Biobank team; in total, 21 and 55 ICs remained, respectively (Alfaro-Almagro et al., 2018). Features were of the following types: **Component Amplitudes**, fluctuation amplitudes (node temporal standard deviation) for each component/node; **Full Correlation Matrix**, correlation-based functional connectivity between each pair of ICs; **Partial Correlation Matrix**, correlation between residues of two independent components after regressing out the other components.

Table 1 summarizes the brain imaging features discussed above together with their references in the UK Biobank.

Controlled variables

We also considered features that might potentially confound the associations with handedness. This group of features included biological sex, age, and genetic information (i.e., the top 10 principal components (PCs) that describe genetic variability in the dataset). It also contained several imaging related variables: imaging assessment center, three scanner-positions, signal-to-noise in T1 and rfMRI, dMRI outlier slices detected and corrected, and rfMRI head motion. We transformed the categorical variable for 'imaging assessment center' into a set of binary dummy variables using one-hot encoding, resulting in a different feature for each center. Table 2 summarizes these controlled variables as well as their corresponding UK Biobank references.

Handedness

Handedness was assessed based on responses to the question: "Are you right- or left-handed?" with 4 response options: "right-handed", "left-handed", "use both right and left equally", and "prefer not to answer". Those who preferred not to answer were excluded from further analysis. Around 89% of the participants were right-handed ($N = 32,090$), while 9% were left-handed ($N = 3374$), and 2% were mixed-handed ($N = 560$). UK Biobank provides handedness information as a categorical attribute with values 0, 1, and 2 being right-handed, left-handed, and mixed-handed respectively; the question was posed via a testing screen when visiting an assessment center. Given the limited sample size of the left- and mixed-handers, in our analysis, we combined left- and mixed-handers into one group, called non-right-hander (Non-RH). Note that this is mainly for maximizing the sample size of the smaller group in the classification, while the left-handers and the mixed-handers sometimes were suggested to have different neuronal and functional correlates (e.g., Annett and Moran, 2006; Badzakova-Trajkov et al., 2011; cf. Hirnstein and Hugdahl, 2014). For a small group of individuals ($N = 216$) having indicated different handedness preference at different visits, we took the most recent measure and thus labelled 84 as right-handers, 132 as non-right-handers. We also ran separate prediction models after excluding people reported as mixed-handed or inconsistently in multiple assessment visits, and the results remained similar.

Machine learning model

Because our handedness variable contains two possible values, namely Non-RH and RH, our learning problem is a binary classification problem. More precisely, we trained logistic regression models to predict handedness based on the aforementioned brain imaging-derived features.

In particular, for each participant i, we have features ($\mathbf{x}^{(i)} := \{x_1^{(i)}, \ldots, x_d^{(i)}\}$) and the participant's handedness binary label ($y^{(i)} = \{0, 1\}$) where 1 indicates being non-right-handed. Let N be the number of participants and $\sigma : \mathrm{R} \to [0, 1]$ be the sigmoid function and $\mathbf{x}^{(i)} \mapsto h(\mathbf{x}^{(i)}) := \beta_0 + \sum_{j=1}^{d} \beta_j x_j^{(i)}$. Predicted probability of being non-right-handed (Non-RH) for each individual i using logistic regression is $\sigma(h(\mathbf{x}^{(i)}))$. Our goal is to estimate the parameters $\{\beta_0, \ldots, \beta_d\}$ of the model such that

$$\underset{\{\beta_0, \ldots, \beta_d\}}{\mathrm{argmin}} - \frac{1}{N} \sum_{i=1}^{N} w^{(i)} [y^{(i)} \log(\sigma(h(\mathbf{x}^{(i)}))) + (1 - y^{(i)}) \log(1 - \sigma(h(\mathbf{x}^{(i)})))]$$

$$+ \frac{1}{C} \sum_{j=1}^{d} \beta_j^2$$

where the first term corresponds to the negative weighted log likelihood of the Bernoulli distribution and the second term corresponds to the l_2 regularization. $w^{(i)}$ is the weight of each i th participant, while C is the hyperparameter (positive real number) penalizing the complexity of the model (i.e., the smaller the value, the higher the penalty). We applied *MinMaxScaler* from scikit-learn (version 0.22.2.post1; https://scikit-learn.org/) (Pedregosa et al., 2011), normalizing each covariate to be between zero and one. The default optimizer implemented in scikit-learn was used to train the logistic regression model. We set the maximum number of optimization iterations at 1000. We also set *class_weight=balanced*, assigning $w^{(i)}$'s to the inverse of the class frequency to which the participant belongs. In other words, participants from the non-right-hander group had larger w_i's than those from the right-hander group, in order to maintain balance at the group level.

Model evaluation and optimization

We used the area under the receiver operating characteristic curve (AUROC) to evaluate the models, computed using scikit-learn. We per-
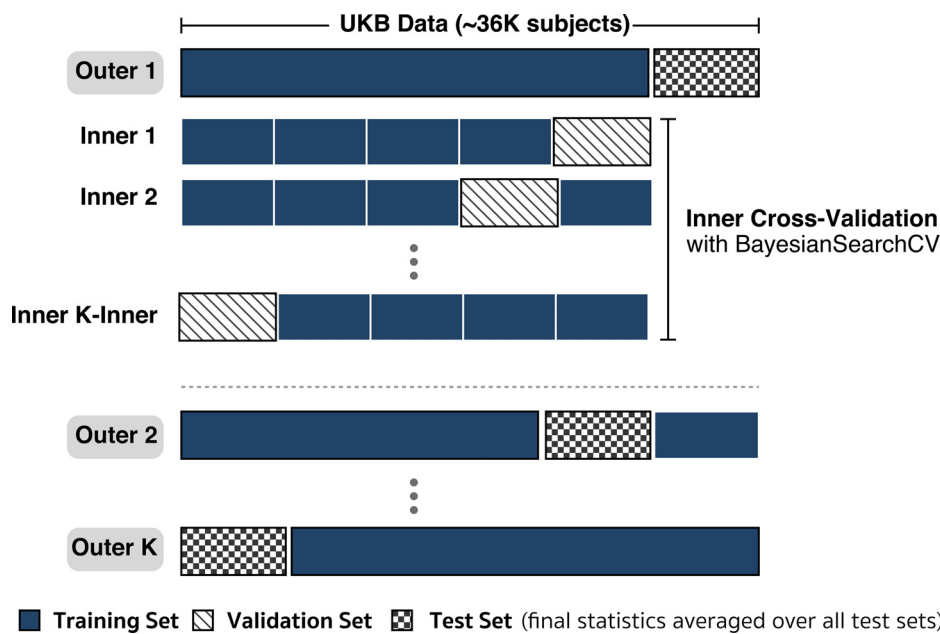
Fig. 1. Nested cross-validation procedure. We perform the procedure to find the value of the regularization hyperparameter and estimate the generalization error (AUROC) of the logistic regression model.

formed nested cross-validation to estimate the AUROC. Unlike standard cross-validation, nested cross-validation has outer and inner loops; the outer loop is responsible for estimating the generalization of our handedness models, while the inner loop is for finding suitable values of hyperparameters; We used BayesianSearchCV from the scikit-optimize package (Head et al., 2020, version 0.7.4) for hyperparameter optimization. Fig. 1 shows the procedures of nested cross-validation. We used 10 fold for the outer loop and 5 fold for the inner loop; we set BayesianSearchCV to sample 5 configurations sequentially.

Methods for feature importance analysis

One aim of this study is to identify the most important imaging features for handedness prediction. A common approach to quantify feature importance is to analyze the weights of the features learned by the model. However, previous work (Haufe et al., 2014; Kriegeskorte and Douglas, 2019) has argued that interpreting weights from linear models could be misleading, e.g., (Haufe et al., 2014) showed a setting in which a model learned a large weight to suppress noise in the data, rather than simply indicating the importance of a given feature.

Another approach is to quantify the importance of each feature by the change in AUROC when excluding that feature, before retraining the model. This approach is similar to the virtual lesion approach (Etzel et al., 2013; Kong et al., 2020b) in neuroscience, or backward feature selection (Guyon and Elisseeff, 2003), or the leave-one-covariate-out approach in machine learning (Lei et al., 2018). For feature importance analysis in the present study, we focused on functional connectivity derived from resting-state fMRI, as this modality showed the largest contribution to handedness prediction (see the Results). The features used in the prediction model were functional connectivity measures between ICs, but we were primarily interested in identifying the ICs themselves that were most important for handedness prediction, not per se the functional connectivities between them. Therefore, separately for each IC, we excluded all connectivity measures with that IC before retraining the model and recording the change in AUROC (Fig. 2).

To present a functional interpretation of the most important features in the prediction, a data-driven decoding analysis was conducted based on a large-scale neuroimaging database (https://neurosynth.org/; version 0.7). Specifically, the "decoder" function from the Neurosynth package was used (Yarkoni et al., 2011). Neurosynth uses text-mining techniques to detect frequently used terms as proxies for functional con-

cepts of interest in thousands of papers from the neuroimaging literature: Terms that occur at a high frequency in a given study are associated with all activation coordinates in that publication, allowing for automated term-based meta-analysis. The decoding analysis ranked the terms in the database by assessing how strongly the meta-analysis map of each functional term correlated with a given map of interest (i.e., in our case the maps for the IC features of interest). There were 590 selected cognitive terms after excluding anatomical (e.g., "hippocampus"), psychiatric (e.g., "autism"), pathological (e.g., "alzheimer"), and non-specific (e.g., "tasks") terms (Karolis et al., 2019). Cognitive terms with a correlation coefficient larger than 0.15 were included in the visualization.

Application of the prediction model to imaging genetics

As an illustration of application of the prediction model, we ran an additional analysis using the predicted probability score derived from the best model (i.e., imaging-derived handedness score). Here we focused on the heritability of handedness, and the genetic correlation between the imaging-derived score and the actual handedness behavioural label. Heritability is a measure ranging from 0 to 1 which indicates the extent to which variation in a trait is influenced by the combined effects of genetic variation over the genome, in this case as captured by common single-nucleotide polymorphisms (SNPs) genotyped in the sample (Vinkhuyzen et al., 2013). Genetic correlation measures the extent to which variability in a pair of traits is influenced by the same genetic variations over the genome. In this study, we hypothesized that the imaging-derived handedness score would show similar heritability to that for the actual handedness, and that the two variables would show high genetic correlation.

To this aim, genotype data from the UK Biobank were used. In brief, in the UK Biobank, 550,192 autosomal, directly genotyped SNPs with minor allele frequencies (MAF) > 0.01, genotyping rate >0.95, and Hardy-Weinberg equilibrium (HWE) $p > 1 \times 10-6$ were used to build a genetic relationship matrix (GRM) using GCTA (version 1.26.0) (Yang et al., 2011). We excluded samples with a genotyping rate of <98% and a kinship coefficient higher than 0.025 based on this GRM, resulting in a sample size of 30,682 participants. Genome-based restricted maximum likelihood (GREML) analyses using GCTA were performed to estimate the SNP-heritabilities for the imaging-derived handedness score as well as the actual handedness label, after residualizing for the
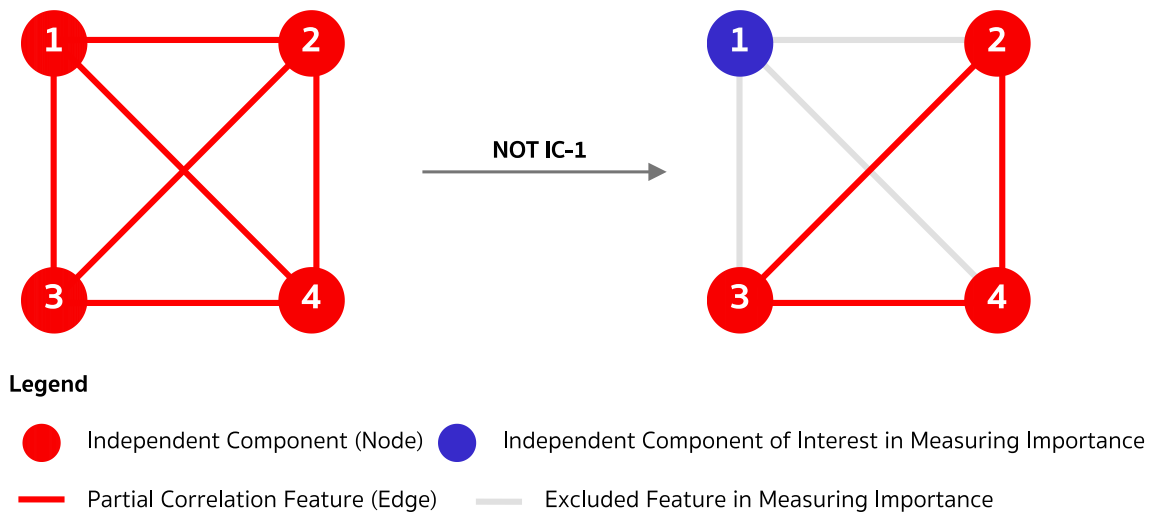
Fig. 2. Schematic to illustrate the virtual lesion approach to determine the importance of a given resting state fMRI-derived independent component (IC) in the prediction model. To determine the importance of IC-1, functional connectivity measures (shown as lines) that are not related to IC-1 are excluded before re-training the model to predict the dependent variable (handedness in our case). The larger the difference in AUROC between the model trained with and without these features, the more important IC-1 is for predicting the dependent variable.

Table 3
Prediction performance of handedness classifiers trained on different sets of brain imaging features. The AUROC of each row is the average of 10 outer-loop statistics from the nested cross validation. Check marks indicate whether the group of features were included in the prediction modeling. Controlled = confounding variables as mentioned in the Methods; structure = brain structural MRI; diffusion = diffusion MRI; rfmri = resting-state fMRI; CA = component amplitude; FC = full correlation-based functional connectivity; PC = partial correlation-based functional connectivity.

Controlled	Structure	Diffusion	rfMRI						AUROC			
			CA-25	FC-25	PC-25	CA-100	FC-100	PC-100	Mean	SD	Min	Max
√									0.5525	0.0120	0.5223	0.5681
	√								0.5539	0.0075	0.5432	0.5642
		√							0.5755	0.0144	0.5490	0.5982
			√						0.5775	0.0134	0.5551	0.5980
				√					0.6556	0.0137	0.6223	0.6732
					√				0.6655	0.0099	0.6423	0.6793
						√			0.5900	0.0164	0.5595	0.6184
							√		0.7001	0.0152	0.6808	0.7294
								√	0.7243	0.0158	0.6944	0.7437
	√	√				√			0.6086	0.0161	0.5813	0.6400
	√	√					√		0.7004	0.0218	0.6660	0.7400
	√	√						√	0.7204	0.0141	0.7016	0.7436
	√	√				√	√		0.7037	0.0146	0.6826	0.7301
	√	√				√		√	0.7231	0.0206	0.6845	0.7471
√	√	√				√		√	0.7234	0.0174	0.6862	0.7422

covariate effects of sex, age, square of z-score of age (z_age2), the first ten PCs capturing genome-wide genetic structure (Bycroft et al., 2018), genotyping array, and several technical variables related to imaging: imaging assessment center (binary), scanner position parameters (continuous X/Y/Z), signal/contrast-to-noise ratio in T1 (continuous), and in-scanner head motion. Bivariate analysis (Lee et al., 2012) were also run in GCTA, to investigate the SNP-based genetic correlation between the handedness measures.

Results

Unimodal models

As baseline for later multimodal analyses, we first trained unimodal logistic regression models on features from each brain imaging modality separately. Table 3 shows that features derived from different brain imaging modalities resulted in various prediction performances, with the rfMRI showing the best results. In particular, among these unimodal models, the model trained with the partial correlation matrix features

derived from 100 independent components (PC-100) achieved the highest AUROC at 0.7243 (SD 0.0158) (Table 3).

The second best unimodal model was the one trained with features from the full correlation matrix features (FC-100) with the same number of components with AUROC at 0.7001 (SD 0.0152). Following these two first models are models that were trained on partial and full correlation matrix features extracted from 25 rfMRI independent components (PC-25 and FC-25 respectively); these models' AUROCs were 0.6655 (SD 0.0099) and 0.6556 (SD 0.0137) respectively.

In contrast, models trained on the other groups of features, namely component amplitude features derived from the rfMRI modality, or diffusion measures, or structure measures, showed AUROC below 0.6. In particular, the least predictive group of features for handedness prediction was the group of structural measures (S), having AUROC at only 0.5539 (SD 0.075), while the controlled group attained AUROC at 0.5525 (SD 0.0120). Taken together, these results suggest that functional measures seem to be more relevant to the inter-individual variations in handedness, at least based on the current set of imaging-derived phenotypes released by the UK Biobank.
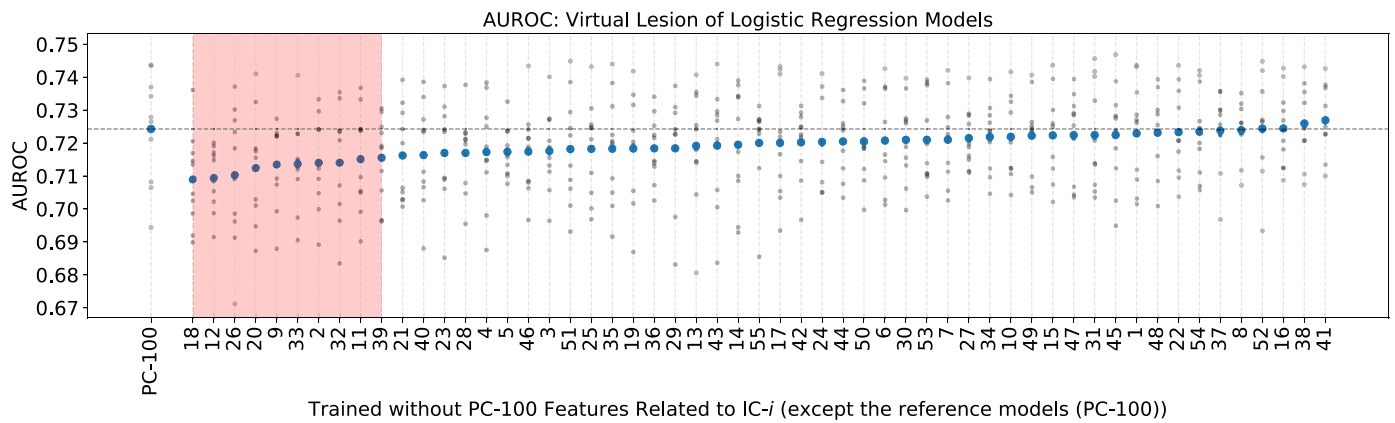
Fig. 3. AUROC of models trained after excluding the features linked to each IC (x- axis). Small dots are AUROC values from the outer loop of the nested cross validation, and the large dots are their average for each IC. The larger difference between the average of the reference model (horizontal dashed line); the more important each IC is. Highlighted area indicates the first 10 models for which the AUROC drops the most.

Multimodal models

We trained models with a combination of features from different modalities. Given that the results of the previous section demonstrated that the models trained on features derived from 100 rfMRI components was always better than using 25 rfMRI components, we focused here on the combination of features from the partial and full correlation matrix extracted from 100 independent components. PC-100 and FC-100 indicate the functional connectivity features calculated using partial correlation and full correlation approaches respectively. Thus, we used features from either one or the other of these two versions in a single analysis, but not both.

As shown in Table 3, the top-performing multimodal model was the model trained on a combination of features derived from the imaging modalities we considered. These features included structure features, diffusion measures, and the rfMRI modality's partial correlation matrix with 100 independent components. This model achieved AUROC at 0.7231 (SD 0.0206), which was slightly lower than the unimodal model being trained only on the rfMRI partial correlation matrix features (PC-100). When using the same combination of features except substituting the features from the partial correlation matrix (PC-100) with the ones from the full correlation matrix (FC-100), we observed a marginal decrease (Table 3).

These results suggest that functional connectivity features derived from resting-date fMRI provide most/all of the information about handedness, relative to brain imaging features from other modalities. In addition, to examine whether controlled variables could impact the prediction, we extended the top-performing multimodal model's features set with the following potential confounding variables (Table 3): age, sex, imaging information (i.e., scanner positions, assessment center, SNRs, head motions), and genetics (via top 10 genotype-based ancestry PCs). Incorporating such variables only slightly increased AUROC further to 0.7234 (SD 0.0174) (Table 3).

Model interpretation

We present the results of the virtual lesion analysis (as described in Methods for Feature Importance Analysis). We used this analysis to quantify the importance of each rfMRI IC in PC-100 for handedness prediction. Together with the importance of each IC, we also present associated brain areas and cognitive terms of a number of important ICs.

Fig. 3's highlighted area shows the first 10 independent components ranked in ascending order by the difference of their AUROCs compared to the reference setting (all features of PC-100). We see that these AUROCs are substantially lower than the one obtained by using all the PC-100 features. In this case, the least predictive setting is the one that excludes features related to IC-18 whose AUROC is at 0.7089 (SD 0.0135); thus, IC-18 seems to contain the most relevant information about handedness among all IC's. The second least predictive setting is when IC-12 linked features were removed whose average AUROC is 0.7093 (SD 0.0092). The rest of Fig. 3 shows that the AUROCs of these virtual lesion models gradually increase and eventually become on par or slightly higher than the reference configuration.

Fig. 4 shows the top 10 functional networks related to the features important for the handedness prediction revealed in the virtual lesion analysis. Interestingly, the most important network (IC-18) showed large overlap with the motor cortex, and the decoding analysis showed clear functional relevance to hand movement. Three other brain networks (IC-20, IC-2, and IC-32) showed similar functional relevance to either hand movement or somatosensory roles. The network of IC-9 showed significant correlation with language-related functions including comprehension. We found four other top networks showing strong right-lateralization (i.e., IC-33, IC-26, IC-11, IC-12), which mainly involved functions such as social interaction, arithmetic, and the default model network. Another network (IC-39) included the frontal eye field and showed relevance to visuospatial attention.

As a control analysis, we also ran the same decoding analysis for the 10 networks with the lowest contributions to handedness prediction (In Supplement, Figure S1). The majority of these features involved early visual or auditory functions: six of them (IC-41, IC-16, IC-52, IC-8, IC-48, and IC-1) showed association with the primary and the ventral visual systems, one with auditory (IC-22), one with reward (IC-38), one for working memory (IC-37), and one with no annotated cognitive terms (IC-54).

Genetic overlap between imaging-derived handedness score and actual handedness

While the performance of the prediction model was not perfect, we found that the imaging-derived handedness score showed a heritability (h^2=7.55%, se=2.12%, $p = 0.000072$) that was similar to, and slightly higher than the actual handedness measure ($h^2 = 6.74\%$, se=2.1%, $p = 0.00090$). Moreover, the imaging-derived handedness score showed high genetic correlation with the actual measure (r_g=0.71, se=0.19, $p = 0.00019$). These results indicate considerable genetic overlap between the imaging-derived handedness score and the actual behavioural measure.

Discussion

Here, we present the largest-ever analysis of handedness in relation to both structural and functional brain organization, making use of data
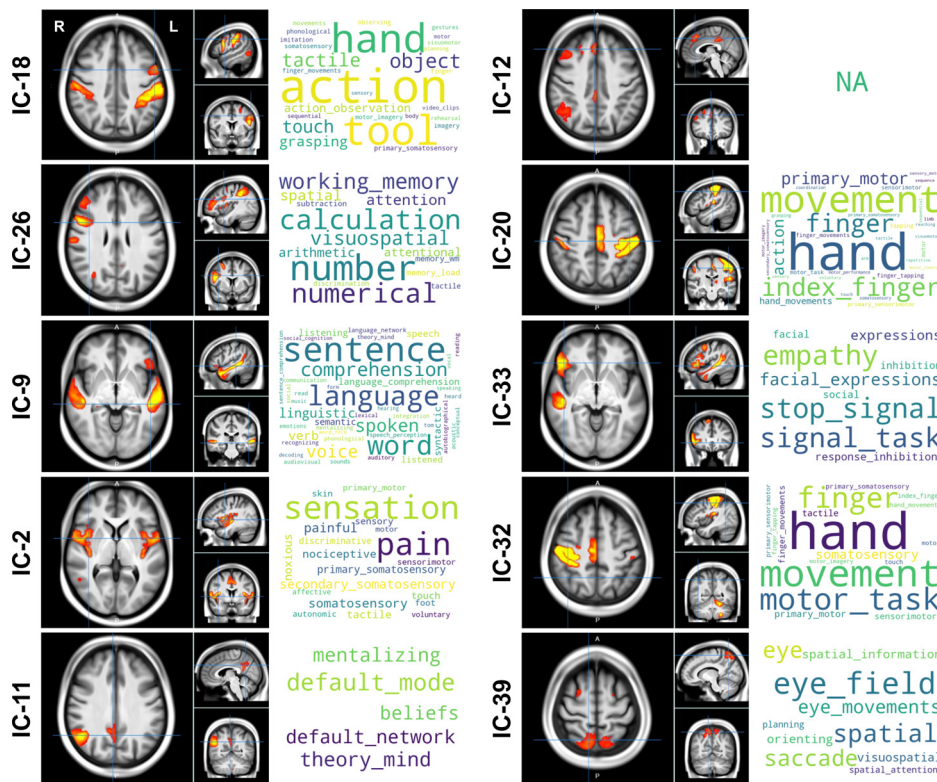
Fig. 4. The top 10 brain networks based on the importance scores obtained by the virtual lesion approach. Cognitive terms revealed in the decoding analysis are shown next to each brain map. Font size indicates the strength of the correlation between the brain map and the activation map relevant to each cognitive term.

from the UK Biobank (N = 36,024). A machine learning approach with multiple modalities of brain imaging data was used to assess whether and to what extent brain imaging data could predict an individual's handedness (i.e., right-handedness versus non-right handedness). Overall, the results showed a good prediction performance, with an AUROC score of up to 0.72. Quantifying the importance of each independent component (IC) using the virtual lesion approach, we found that the top components describe intrinsic functional networks for hand movement and higher-level cognitive functions such as language comprehension, arithmetic, and social interaction. Further genetic analyses of the imaging-derived handedness score using the prediction model showed similar heritability to the actual handedness measure, as well as high genetic correlation between the two.

Handedness and multimodal brain imaging

For years, there has been great interest in the relationship between handedness and the brain, but mostly a small sample size and/or one single imaging modality was used (see Introduction). These existing studies were usually based on univariate approaches, such as correlation and generalized linear models. While these studies indeed provided new insights in the neurobiological basis of handedness, the effect sizes of these univariate analyses were usually low (Kong et al., 2018, 2022; Carrion-Castillo, 2020). In a recently published study, Sha and colleagues mapped cortical morphometry differences (i.e., thickness and surface area asymmetry) associated with handedness in the UK Biobank, and revealed a number of significant clusters, all of which also showed small effect sizes (Cohen's $d < 0.1$) (Sha et al., 2021). In the present study, we for the first time took advantage of multimodal imaging data in the UK Biobank, and combined it with a multivariate machine learning approach to explore how and to what extent the brain imaging data could predict an individual's handedness. Overall, the best model resulted in a good prediction performance with an AUROC of up to 0.72. In addition, we found that the prediction accuracy was similar after controlling for the confounding factors such as age, sex, potential heterogeneity in brain imaging, head motion during scanning, and

population structure, suggesting that predictive modeling is largely insensitive to such factors.

In line with this, in the unimodal modeling analysis, we found that models based on the functional connectivity measures showed much higher performance (AUROC=0.6556–0.7243), compared with those based on structural measures of gray matter (AUROC=0.5539) and white matter (AUROC=0.5755). In fact the latter models performed only slightly higher than chance level (AUROC=0.5). These results are broadly consistent with previous findings of small effect sizes for univariate associations between handedness and highly localized gray matter measures (Sha et al., 2021), while measures of relatively large regions as defined in the Desikan atlas (as used in the present study) have also shown a lack of association with handedness in another large-scale study via the ENIGMA (Enhancing Neuro-Imaging Genetics through Meta-Analysis) consortium (Kong et al., 2018).

More intriguingly, the virtual lesion approach and the decoding analysis suggest that the brain networks for cognitive functions including language-related functions, visuospatial attention, arithmetic, and social interaction and the default mode network, along with the networks for handedness movement (for details see Fig. 4), were most related to handedness. These results seem to be in line with recent findings that handedness-related differences were found in brain regions/networks for hand control, language, and visual functions (Sha et al., 2021; Wiberg et al., 2019). The present study provides new evidence supporting such associations, but also suggests novel links of handedness with brain networks for number processing and social functions, and the default mode network. Together, these results suggest that analysis of multivariate machine learning modeling of brain imaging measures could provide a more comprehensive picture of neurobiological basis of handedness.

Handedness and brain imaging genetics

Previous studies have shown that genetic variation contributes modestly to handedness, with heritability estimates ranging from 3% for SNP-based heritability in the UK Biobank (N > 108,000) (Ge et al.,

2017), to 25% in twin studies (Medland et al., 2009). A recent study in the UK Biobank suggested that some genetic loci associated with handedness are associated with individual variation in cortical structural asymmetries that showed significant differences in left-handers (Sha et al., 2021). Here, we found that the imaging-derived handedness score showed similar heritability to the actual behavioural measure (around 7%). More interestingly, we found that the imaging-derived handedness score showed high genetic correlation with the handedness behavioural measure ($rg = 0.71$), suggesting considerable overlap in the underlying genetic variation. Compared with the modest performance of the handedness prediction model, the high genetic correlation between the predicted score and the actual handedness measure suggests that the imaging-derived score largely retains the variance in handedness that is due to genetic factors.

Moreover, with handedness as an example trait of interest, our results suggest that a predictive model approach based on brain data could provide a proxy of behavioural observations for future large-scale imaging genetics studies. Hand preference itself is relatively easy to measure in large samples (e.g., the sample size of the largest genome-wide association study to date was over 1.7 million) (Cuellar-Partida et al., 2021). Nonetheless, the approach adopted here could be particularly useful when large-scale brain imaging data has already been collected e.g., in a psychiatry department, without much relevant behavioural data such as handedness. For instance, in the ENIGMA consortium (Thompson et al., 2020), tens of thousands of MRI images have been collated via multi-site collaboration (e.g., Grasby et al., 2020), but relatively few sites have collected comparable indexes of individual's cognition and behavior, which limits large-scale studies linking human cognition, brain and genes. In addition, it is interesting in the future to explore the links of the imaging-derived handedness score with other behavioural variables that informs brain laterality when such variables are available.

Limitations and future directions

It is important to note that the assessment of hand preference in the UK Biobank was by a simple question (i.e., "Are you right- or left-handed?") and thus is less than ideal. Simple assessments such as this have been shown to capture an inherent dichotomy in hand preference that is also revealed by more quantitative, multi-term questionnaires (Ransil and Schachter 1994). However, the results may have been different if using performance-based hand skill measures or multi-item handedness ratings which further reflect the strength of hand preference (Crow et al., 1998). People using both hands equally may form a somewhat distinct category with respect to behavioural and brain correlates (Badzakova-Trajkov et al., 2011). We also ran a separate prediction model after excluding people having reported as mixed-handed, and obtained very similar results in both prediction performance (0.7360 versus the original 0.7243) and the importance of the ICs ($r = 0.62$, $p = 5.73e-07$). Similarly, functions suggested by the decoding analyses of the top IC networks showed much overlap with those in the main analyses, which included functions including hand movement, language-related functions, calculation, social interaction and visuospatial functions. These results suggested that the present results were mainly contributed by the differences between the left- and right-handers. In addition, when possible, future studies should investigate the reliability and robustness of the results, e.g., via the ENIGMA Laterality working group (Thompson et al., 2020; Kong et al., 2022).

This study has several points that could be improved to possibly achieve a better prediction performance for hand preference. First, lateralization has been observed widely in the cognitive, emotional, and language systems. Task fMRI for these domains could provide useful information to enhance the prediction. However, in the UK Biobank, only a few tasks were included for fMRI experiments. We would expect that further task-related phenotypes could provide useful information for the prediction. New phenotype discovery approaches which inte-

grate decomposition algorithms and multimodal features could also be considered (Gong et al., 2021).

Secondly, it should be noted that the structure and diffusion features were atlas-based while the rfMRI features were data-driven (the latter from ICA). As most of the predictive power for handedness in this study was derived from the rfMRI measures, with minimal contributions from the other modalities, the utility of a multi-modal approach was not clearly illustrated in this specific application. However, using a vertex-based (atlas-free) approach for computing structure symmetries, Sha et al. (2021) recently found a number of cortical regional asymmetries that associate with hand preference, which were generally smaller and more focal than the Desikan-Killiany atlas regions as used in the present study. Future work should investigate whether atlas-free approaches to structure and diffusion features can help to further improve handedness prediction in combination with rfMRI measures.

Lastly, assembling models (e.g., random forest) and more complex machine learning approaches such as artificial neural networks could provide better prediction performance; however, one potential challenge in that setting is extracting scientific insight from these complex models. One could overcome such an interpretability challenge by utilizing recent developments in explanation methods (Samek, 2019), e.g., Layer-wise Relevance Propagation (Bach et al., 2015), that can produce explanation for predictions from these complex models. In addition, polygenic scores for handedness (Cuellar-Partida et al., 2021; Wiberg et al., 2019) and early life factors associated with handedness (de Kovel and Francks, 2019), could also be considered.

Conclusion

In sum, we present the largest-ever analysis of handedness in relation to multimodal brain imaging features, by applying multivariate machine learning approaches in the UK Biobank. Overall, the results showed a good prediction performance, with an AUROC score of up to 0.7243 (SD 0.0158); the most predictive features were related to functional connectivity of the brain networks derived from resting-state functional MRI. Our virtual lesion analysis and decoding analysis for ranking the importance of the brain networks in the handedness prediction revealed networks relevant for hand movement as well as for higher-level cognitive functions such as language-related functions (except for visual processing of words), arithmetic, and social interaction. While these results are correlational and based on older adults, new possibilities on the neural and cognitive correlates of handedness development were suggested. Further genetic analyses of the imaging-derived handedness score using the prediction model showed similar heritability to the actual handedness measure, and also showed high genetic correlation with the actual measure, suggesting that the imaging-derived score largely maintained the heritable variance in handedness.

Competing interests

The authors indicate no competing interest.

Author contributions

P.C.: study conception and design, data preparation, model training, analysis, visualization, and preparing the first draft; Y.P.: study conception, data analysis, and editing the manuscript; H.H.: data analysis, visualization, and editing the manuscript; S.E.F: study conception and design, editing the manuscript; C.F.: data provision, study conception and design, editing the manuscript; X.K.: study conception and design, data preparation, analysis, visualization, preparing the first draft and editing.

Data and code availability

Our study primarily relies on the dataset provided by the UK Biobank, which is made available to all qualified researchers via their

website https://www.ukbiobank.ac.uk/ . We provide our code for model training and training statistics at https://osf.io/4q87k/. Our computation and analysis was conducted using the computational cluster of Max Planck Institute for Psycholinguistics, Nijmegen, The Netherlands.

Data availability

The authors do not have permission to share data.

Acknowledgements

Supplementary materials

Supplementary material associated with this article can be found, in the online version, at doi:10.1016/j.neuroimage.2022.119534.

References

Alfaro-Almagro, F., Jenkinson, M., Bangerter, N.K., Andersson, J.L.R., Griffanti, L., Douaud, G., Sotiropoulos, S.N., Jbabdi, S., Hernandez-Fernandez, M., Vallee, E., Vidaurre, D., Webster, M., McCarthy, P., Rorden, C., Daducci, A., Alexander, D.C., Zhang, H., Dragonu, I., Matthews, P.M., … Smith, S.M., 2018. Image processing and Quality Control for the first 10,000 brain imaging datasets from UK Biobank. Neuroimage 166, 400–424. doi:10.1016/j.neuroimage.2017.10.034.

Annett, M., 1970. A classification of hand preference by association analysis. Br. J. Psychol. 61 (3), 303–321.

Annett, M., Moran, P., 2006. Schizotypy is increased in mixed-handers, especially right-handed writers who use the left hand for primary actions. Schizophr. Res. 81, 239–246.

Bach, S., Binder, A., Montavon, G., Klauschen, F., Müller, K.-R., Samek, W., 2015. On pixel-wise explanations for non-linear classifier decisions by layer-wise relevance propagation. PLoS ONE 10 (7), e0130140. doi:10.1371/journal.pone.0130140.

Badzakova-Trajkov, G., Häberling, I.S., Corballis, M.C., 2011. Magical ideation, creativity, handedness, and cerebral asymmetries: a combined behavioural and fMRI study. Neuropsychologia 49, 2896–2903.

Bycroft, C., Freeman, C., Petkova, D., Band, G., Elliott, L.T., Sharp, K., Motyer, A., Vukcevic, D., Delaneau, O., O'Connell, J., Cortes, A., Welsh, S., Young, A., Effingham, M., McVean, G., Leslie, S., Allen, N., Donnelly, P., Marchini, J., 2018. The UK Biobank resource with deep phenotyping and genomic data. Nature 562 (7726), 203–209. doi:10.1038/s41586-018-0579-z.

Budisavljevic, S., Castiello, U., Begliomini, C., 2020. Handedness and white matter networks. Neuroscientist 1073858420937657. doi:10.1177/1073858420937657.

Bzdok, D., Meyer-Lindenberg, A., 2018. Machine learning for precision psychiatry: opportunities and challenges. Biol. Psychiatry Cogn. Neurosci. Neuroimag. 3, 223–230.

Canario, E., Chen, D., Biswal, B., 2021. A review of resting-state fMRI and its use to examine psychiatric disorders. Psychoradiology 1, 42–53.

Crow, T.J., Crow, L.R., Done, D.J., Leask, S., 1998. Relative hand skill predicts academic ability: global deficits at the point of hemispheric indecision. Neuropsychologia 36, 1275–1282.

Cuellar-Partida, G., Tung, J.Y., Eriksson, N., Albrecht, E., Aliev, F., Andreassen, O.A., Barroso, I., Beckmann, J.S., Boks, M.P., Boomsma, D.I., Boyd, H.A., Breteler, M.M.B., Campbell, H., Chasman, D.I., Cherkas, L.F., Davies, G., de Geus, E.J.C., Deary, I.J., Deloukas, P., … Medland, S.E., 2021. Genome-wide association study identifies 48 common genetic variants associated with handedness. Nature Human Behaviour 5 (1), 59–70. doi:10.1038/s41562-020-00956-y.

Carrion-Castillo, Amaia, et al., 2020. Genetic effects on planum temporale asymmetry and their limited relevance to neurodevelopmental disorders, intelligence or educational attainment. Cortex 124. doi:10.1016/j.cortex.2019.11.006.

Corballis, M.C., 2003. From mouth to hand: gesture, speech, and the evolution of right-handedness. Behav. Brain Sci. 26 (2), 199–208.

de Kovel, C.G.F., Francks, C., 2019. The molecular genetics of hand preference revisited. Sci Rep 9 (1), 5986. doi:10.1038/s41598-019-42515-0.

Etzel, J.A., Zacks, J.M., Braver, T.S., 2013. Searchlight analysis: promise, pitfalls, and potential. Neuroimage 78, 261–269.

Fischl, B., 2012. FreeSurfer. Neuroimage 62 (2). doi:10.1016/j.neuroimage.2012.01.021.

Frässle, S., Krach, S., Paulus, F.M., Jansen, A., 2016. Handedness is related to neural mechanisms underlying hemispheric lateralization of face processing. Sci. Rep. 6 (1), 1–17.

Ge, T., Chen, C.-Y., Neale, B.M., Sabuncu, M.R., Smoller, J.W., 2017. Phenome-wide heritability analysis of the UK Biobank. PLoS Genet. 13.

Germann, J., Petrides, M., Chakravarty, M.M., 2019. Hand preference and local asymmetry in cerebral cortex, basal ganglia, and cerebellar white matter. Brain Struct. Funct. 224 (8), 2899–2905. doi:10.1007/s00429-019-01941-6.

Gong, W., Beckmann, C.F., Smith, S.M., 2021. Phenotype discovery from population brain imaging. Medical Image Analysis doi:10.1016/j.media.2021.102050.

Grasby, K.L., Jahanshad, N., Painter, J.N., Colodro-Conde, L., Bralten, J., Hibar, D.P., Lind, P.A., Pizzagalli, F., Ching, C.R.K., McMahon, M.A.B., Shatokhina, N., Zsembik, L.C.P., Thomopoulos, S.I., Zhu, A.H., Strike, L.T., Agartz, I., Alhusaini, S., Almeida, M.A.A., … Alnæs, D., 2020. The genetic architecture of the human cerebral cortex. Science 367 (6484), eaay6690. doi:10.1126/science.aay6690.

Guadalupe, T., Willems, R.M., Zwiers, M.P., Arias Vasquez, A., Hoogman, M., Hagoort, P., Fernandez, G., Buitelaar, J., Franke, B., Fisher, S.E., Francks, C, 2014. Differences in cerebral cortical anatomy of left- and right-handers. Front. Psychol. 5, 261. doi:10.3389/fpsyg.2014.00261.

Guyon, I., Elisseeff, A., 2003. An introduction to variable and feature selection. J. Mach. Learn. Res. 3 (Mar), 1157–1182.

Haufe, S., Meinecke, F., Görgen, K., Dähne, S., Haynes, J.-D., Blankertz, B., Bießmann, F., 2014. On the interpretation of weight vectors of linear models in multivariate neuroimaging. Neuroimage 87, 96–110.

Head, T., Kumar, M., Nahrstaedt, H., Louppe, G., Shcherbatyi, I., 2020. Scikit-optimize/scikit-optimize (v0.7.4) [Computer software]. Zenodo doi:10.5281/zenodo.1157319.

Hirnstein, M., Hugdahl, K., 2014. Excess of non-right-handedness in schizophrenia: meta-analysis of gender effects and potential biases in handedness assessment. Br. J. Psychiatry 205 (4), 260–267. doi:10.1192/bjp.bp.113.137349.

Hyvärinen, A., Oja, E., 2000. Independent component analysis: algorithms and applications. Neural Netw. 13 (4–5), 411–430. doi:10.1016/S0893-6080(00)00026-5.

Karolis, V.R., Corbetta, M., de Schotten, M.T., 2019. The architecture of functional lateralisation and its relationship to callosal connectivity in the human brain. Nat. Commun. 10 (1), 1–9.

Kong, Xiang-Zhen, Francks, ClydeENIGMA Laterality Working Group, 2022. Reproducibility in the absence of selective reporting: An illustration from large-scale brain asymmetry research. Human Brain Mapping 43 (1). doi:10.1002/hbm.25154.

Kong, X.-Z., Mathias, S.R., Guadalupe, T., Glahn, D.C., Franke, B., Crivello, F., Tzourio-Mazoyer, N., Fisher, S.E., Thompson, P.M., Francks, C., 2018. Mapping cortical brain asymmetry in 17,141 healthy individuals worldwide via the ENIGMA Consortium. Proc. Natl. Acad. Sci. 115 (22), E5154–E5163. doi:10.1073/pnas.1718845115.

Kong, X.-Z., Postema, M.C., Guadalupe, T., de Kovel, C., Boedhoe, P.S.W., Hoogman, M., Mathias, S.R., van Rooij, D., Schijven, D., Glahn, D.C., Medland, S.E., Jahanshad, N., Thomopoulos, S.I., Turner, J.A., Buitelaar, J., van Erp, T.G.M., Franke, B., Fisher, S.E., van den Heuvel, O.A., … Francks, C., 2022. Mapping brain asymmetry in health and disease through the ENIGMA consortium. Hum. Brain Mapp. 43 (1), 167–181. doi:10.1002/hbm.25033.

Kong, X.-Z., Tzourio-Mazoyer, N., Joliot, M., Fedorenko, E., Liu, J., Fisher, S.E., Francks, C., 2020b. Gene expression correlates of the cortical network underlying sentence processing. Neurobiol. Lang. 1 (1), 77–103. doi:10.1162/nol_a_00004.

Kong, X.-Z., Postema, M., Schijven, D., Castillo, A.C., Pepe, A., Crivello, F., Joliot, M., Mazoyer, B., Fisher, S.E., Francks, C., 2021. Large-scale phenomic and genomic analysis of brain asymmetrical skew. Cereb. Cortex 31 (9), 4151–4168. doi:10.1093/cercor/bhab075.

Kong, X.Z., Wang, X., Pu, Y., Huang, L., Hao, X., Zhen, Z., Liu, J., 2017. Human navigation network: the intrinsic functional organization and behavioral relevance. Brain Struct. Funct. 222, 749–764.

Kriegeskorte, N., Douglas, P.K., 2019. Interpreting encoding and decoding models. Curr. Opin. Neurobiol. 55, 167–179.

Lee, S.H., Yang, J., Goddard, M.E., Visscher, P.M., Wray, N.R., 2012. Estimation of pleiotropy between complex diseases using single-nucleotide polymorphism-derived genomic relationships and restricted maximum likelihood. Bioinformatics 28 (19), 2540–2542. doi:10.1093/bioinformatics/bts474.

Lei, J., G'Sell, M., Rinaldo, A., Tibshirani, R.J., Wasserman, L, 2018. Distribution-free predictive inference for regression. J. Am. Stat. Assoc. 113 (523), 1094–1111.

Li, F., Sun, H., Biswal, B.B., Sweeney, J.A., Gong, Q., 2022. Artificial intelligence applications in psychoradiology. Psychoradiology 1, 94–107.

Logue, D.D., Logue, R.T., Kaufmann, W.E., Belcher, H.M.E., 2015. Psychiatric disorders and left-handedness in children living in an urban environment. Laterality 20, 249–256.

Maingault, S., Tzourio-Mazoyer, N., Mazoyer, B., Crivello, F., 2016. Regional correlations between cortical thickness and surface area asymmetries: a surface-based morphometry study of 250 adults. Neuropsychologia 93, 350–364. doi:10.1016/j.neuropsychologia.2016.03.025.

Marek, S., Tervo-Clemmens, B., Calabro, F.J., Montez, D.F., Kay, B.P., Hatoum, A.S., Donohue, M.R., Foran, W., Miller, R.L., Hendrickson, T.J., Malone, S.M., Kandala, S., Feczko, E., Miranda-Dominguez, O., Graham, A.M., Earl, E.A., Perrone, A.J., Cordova, M., Doyle, O., Moore, L.A., Conan, G.M., Uriarte, J., Snider, K., Lynch, B.J., Wilgenbusch, J.C., Pengo, T., Tam, A., Chen, J., Newbold, D.J., Zheng, A., Seider, N.A., Van, A.N., Metoki, A., Chauvin, R.J., Laumann, T.O., Greene, D.J., Petersen, S.E., Garavan, H., Thompson, W.K., Nichols, T.E., Yeo, B.T.T., Barch, D.M., Luna, B., Fair, D.A., Dosenbach, N.U.F., 2022. Reproducible brain-wide association studies require thousands of individuals. Nature 603, 654–660.

Marie, D., Jobard, G., Crivello, F., Perchey, G., Petit, L., Mellet, E., Joliot, M., Zago, L., Mazoyer, B., Tzourio-Mazoyer, N., 2015. Descriptive anatomy of Heschl's gyri in 430

healthy volunteers, including 198 left-handers. Brain Struct. Funct. 220 (2), 729–743. doi:10.1007/s00429-013-0680-x.

Markou, P., Ahtam, B., Papadatou-Pastou, M., 2017. Elevated levels of atypical handedness in autism: meta-analyses. Neuropsychol. Rev. 27 (3), 258–283. doi:10.1007/s11065-017-9354-4.

Mascie-Taylor, C.G.N., 1981. Hand preference and personality traits. Cortex 17 (2), 319–322. doi:10.1016/S0010-9452(81)80052-4.

Mazoyer, B., Zago, L., Jobard, G., Crivello, F., Joliot, M., Perchey, G., Mellet, E., Petit, L., Tzourio-Mazoyer, N., 2014. Gaussian mixture modeling of hemispheric lateralization for language in a large sample of healthy individuals balanced for handedness. PLoS ONE 9 (6), e101165. doi:10.1371/journal.pone.0101165.

McManus, C., 2022. Cerebral polymorphisms for Lateralisation: modelling the genetic and phenotypic architectures of multiple functional modules. Symmetry-Basel 14.

Medland, S.E., Duffy, D.L., Wright, M.J., Geffen, G.M., Hay, D.A., Levy, F., van-Beijsterveldt, C.E.M., Willemsen, G., Townsend, G.C., White, V., Hewitt, A.W., Mackey, D.A., Bailey, J.M., Slutske, W.S., Nyholt, D.R., Treloar, S.A., Martin, N.G., Boomsma, D.I., 2009. Genetic influences on handedness: data from 25,732 Australian and Dutch twin families. Neuropsychologia 47 (2), 330–337. doi:10.1016/j.neuropsychologia.2008.09.005.

Miller, Karla L, Alfaro-Almagro, Fidel, Bangerter, Neal K, Thomas, David L, et al., 2016. Multimodal population brain imaging in the UK Biobank prospective epidemiological study. Nat Neurosci 9 (11). doi:10.1038/nn.4393.

Nastou, E., Ocklenburg, S., Hoogman, M., Papadatou-Pastou, M., 2022. Handedness in ADHD: meta-analyses. Neuropsychol. Rev.

Oldfield, R.C., 1971. The assessment and analysis of handedness: the edinburgh inventory. Neuropsychologia 9 (1), 97–113.

Packheiser, J., Schmitz, J., Stein, C.C., Pfeifer, L.S., Berretz, G., Papadatou-Pastou, M., Peterburs, J., Ocklenburg, S., 2021. Handedness and depression: a meta-analysis across 87 studies. J. Affect. Disord. 294, 200–209.

Panta, S.R., Anderson, N.E., Maurer, J.M., Harenski, K.A., Nyalakanti, P.K., Calhoun, V.D., Kiehl, K.A., 2021. Classifying handedness with MRI. Neuroimage: Reports 1 (4), 100057. doi:10.1016/j.ynirp.2021.100057.

Pedregosa, F., Varoquaux, G., Gramfort, A., Michel, V., Thirion, B., Grisel, O., Duchesnay, E., 2011. Scikit-learn: machine learning in Python. J. Mach. Learn. Res. 12, 2825–2830.

Peters, M., Reimers, S., Manning, J.T., 2006. Hand preference for writing and associations with selected demographic and behavioral variables in 255,100 subjects: the BBC internet study. Brain Cogn. 62 (2), 177–189. doi:10.1016/j.bandc.2006.04.005.

Ransil, B.J., Schachter, S.C., 1994. Test-retest reliability of the Edinburgh Handedness Inventory and Global Handedness preference measurements, and their correlation. Percept. Mot. Skills 79, 1355–1372.

Samek, W., 2019. Explainable AI: interpreting, Explaining and Visualizing Deep Learning. Springer, Nature (Vol. 11700).

Sha, Z., Pepe, A., Schijven, D., Carrión-Castillo, A., Roe, J.M., Westerhausen, R., Joliot, M., Fisher, S.E., Crivello, F., Francks, C., 2021. Handedness and its genetic influences are associated with structural asymmetries of the cerebral cortex in 31,864 individuals. Proc. Natl. Acad. Sci. 118 (47). doi:10.1073/pnas.2113095118.

Sudlow, Cathie, Gallacher, John, Allen, Naomi, Beral, Valerie, Burton, Paul, Danesh, John, Downey, Paul, Elliott, Paul, Green, Jane, Landray, Martin, Liu, Bette, Matthews, Paul, Ong, Giok, Collins, Rory, 2015. UK biobank: an open access resource for identifying the causes of a wide range of complex diseases of middle and old age. PLoS Medicine 12 (3). doi:10.1371/journal.pmed.1001779.

Thompson, P.M., Jahanshad, N., Ching, C.R.K., Salminen, L.E., Thomopoulos, S.I., Bright, J., Baune, B.T., Bertolín, S., Bralten, J., Bruin, W.B., Bülow, R., Chen, J., Chye, Y., Dannlowski, U., de Kovel, C.G.F., Donohoe, G., Eyler, L.T., Faraone, S.V., … Favre, P., 2020. ENIGMA and global neuroscience: a decade of large-scale studies of the brain in health and disease across more than 40 countries. Transl Psychiatry 10 (1), 100. doi:10.1038/s41398-020-0705-1.

Toga, A.W., Thompson, P.M., 2003. Mapping brain asymmetry. Nat. Rev. Neurosci. 4 (1), 37–48. doi:10.1038/nrn1009.

Tzourio-Mazoyer, N., Labache, L., Zago, L., Hesling, I., Mazoyer, B., 2021. Neural support of manual preference revealed by BOLD variations during right and left finger-tapping in a sample of 287 healthy adults balanced for handedness. Laterality 26 (4). doi:10.1080/1357650X.2020.1862142.

Vinkhuyzen, A.A.E., Wray, N.R., Yang, J., Goddard, M.E., Visscher, P.M., 2013. Estimation and partition of heritability in human populations using whole-genome analysis methods. Annu. Rev. Genet. 47, 75–95. doi:10.1146/annurev-genet-111212-133258.

Wiberg, A., Ng, M., Al Omran, Y., Alfaro-Almagro, F., McCarthy, P., Marchini, J., Bennett, D.L., Smith, S., Douaud, G., Furniss, D., 2019. Handedness, language areas and neuropsychiatric diseases: insights from brain imaging and genetics. Brain 142 (10), 2938–2947.

Yang, J., Lee, S.H., Goddard, M.E., Visscher, P.M., 2011. GCTA: a tool for genome-wide complex trait analysis. Am. J. Hum. Genetic. 88 (1), 76–82. doi:10.1016/j.ajhg.2010.11.011.

Yarkoni, T., Poldrack, R.A., Nichols, T.E., Van Essen, D.C., Wager, T.D., 2011. Large-scale automated synthesis of human functional neuroimaging data. Nat. Methods 8 (8), 665–670. doi:10.1038/nmeth.1635.